03

Spectra of optical effects in magnetic fluids containing nanoparticle aggregates

© V.I. Vivchar, K.V. Yerin*

North-Caucasian Federal University,
355017 Stavropol, Russia
e-mail: exiton@inbox.ru

Received February 16, 2023
Revised March 14, 2023
Accepted March 14, 2024

The spectra of the optical effects of birefringence, dichroism, and changes in transparency in a magnetic fluid with nanoparticle aggregates arising under the influence of a magnetic field have been studied. Based on experimental data, the spectral dependences of the complex refractive index of aggregates of magnetite nanoparticles were determined. An interpretation of changes in the shape of the transmission spectra of aggregated magnetic fluids under the influence of a magnetic field and temperature is proposed..

Keywords: magnetic fluids, transparency change, birefringence, dichroism, nanoparticles aggregates.

DOI: 10.61011/EOS.2024.03.58754.6046-23

Introduction

Stable colloidal solutions of ferro- and ferrimagnetic nanoparticles in various organic and inorganic fluids are commonly called magnetic fluids [1]. Following their discovery in the late 1960s, these systems have found various applications in technology, instrumentation engineering, and biomedicine [2]. A number of optical effects may be observed in magnetic fluids under the influence of magnetic and electric fields: birefringence [3], dichroism [4], Faraday rotation [5], and variation of intensity of scattered and reflected light [6,7]. The first theoretical interpretations of these effects were based on the traditional (for colloidal systems) concept of orientational ordering of long axes of non-spherical particles under the influence of a field. In the context of optical effects, this approach is called the orientational model of optical anisotropy [8].

Experiments [9,10] and computer modeling [11,12] have revealed a significant influence of particle aggregates on the physical properties of magnetic fluids. There is currently no doubt that the aggregation of nanoparticles of magnetic fluids, the formation of microstructure of such systems, and their colloidal stability are governed by the balance of attraction (due to van der Waals forces and magnetic dipole-dipole interaction) and steric repulsion of the adsorption shells of particles. Aggregates of two main types are observed in magnetic fluids exposed to a magnetic field: chain aggregates, which are elongated structures of several particles, and microdroplet ones, which form as a result of a singular „gas – liquid“ first-order phase transition. Microdroplet aggregates are regions of high concentration of nanoparticles separated by a clear boundary with surface tension from the surrounding colloid with a low particle concentration. The interphase surface properties are largely governed by interparticle interactions [13]. Violation of the aggregative stability of magnetic fluids affects their optical properties. Particle aggregates increase significantly the magnitude and the relaxation time of birefringence [8] and induce anisotropic light scattering [14] and changes in transparency [15] or even the color (magnetochromatic effect) [16] of colloidal systems.

Intriguing practical applications of optical effects in magnetic fluids involving the determination of organic and inorganic compounds by changes in transmission spectra [17] and the fabrication of ultra-sensitive magnetic field sensors with a magnetic fluid deposited on the surface of optical fiber [18] have been proposed recently. Data on the spectra of optical parameters of nanoparticle aggregates are needed to advance these techniques and construct correct models of optical effects in aggregated magnetic fluids.

In the present study, we report on the results of examination of the spectra of optical effects (changes in transparency, birefringence, and dichroism) and determination of the optical characteristics of a magnetic fluid based on kerosene with magnetite nanoparticles, which form aggregates up to 100–150 nm in size under the influence of a magnetic field.

Experiment

A „magnetite in kerosene“ magnetic fluid produced by STC Magnetic Fluids (Naro-Fominsk, Russia) with an average radius of magnetite particles of 13.7 nm and oleic acid used as a stabilizer was examined. The volume concentration of the initial fluid is 10%. Samples with a volume concentration of 0.05–0.1% were obtained by diluting the initial fluid with TS-1 kerosene. Dynamic and static light scattering studies performed using a PhotocorComplex analyzer demonstrated that particle aggregates up to 100 nm

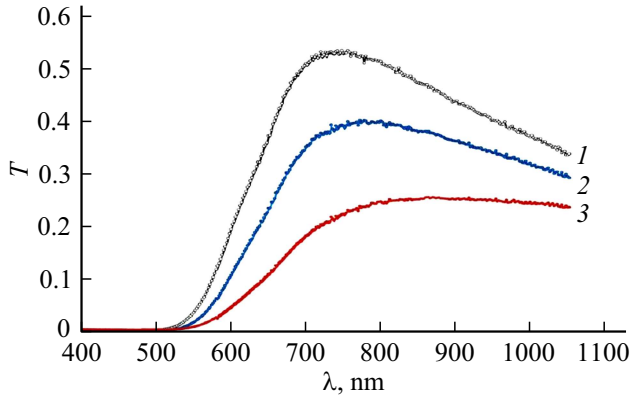

Figure 1. Transmission spectra of a magnetic fluid with a concentration of 0.05% in a 5-mm-thick cell without a magnetic field (*1*) and in magnetic field $H = 10$ (*2*) and 20 kA/m (*3*).

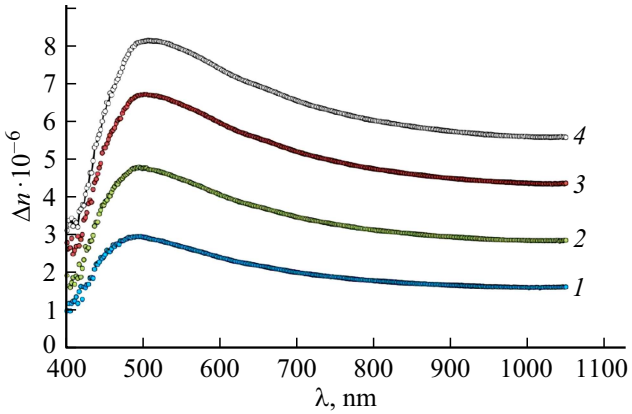

Figure 2. Spectra of birefringence in a magnetic fluid with a concentration of 0.05% at $H = 5$ (*1*), 9 (*2*), 13 (*3*), and 20 kA/m (*4*).

in size form in samples under the influence of a magnetic field with an approximate intensity of 15 kA/m.

Transmission spectra of the magnetic fluid were measured with an „ Ellips-1891“ spectral ellipsometric complex in transmitted light within the 350–1050 nm wavelength range. An electromagnet was used to produce a magnetic field perpendicular to the light beam; the sample under study was positioned in a cell with thickness l in a region of a uniform magnetic field. Spectral dependences of transparency in unpolarized light ($T = I/I_0$) and ellipsometric angles Δ and ψ of the polarization ellipse of transmitted light were measured. The tangent of angle ψ specifies the ratio of attenuations of scalar amplitudes of s and p components in transmission, while angle Δ specifies the difference in phase shifts in transmission of radiation with s and p polarization states. The complex transmittance may then also be written in the form of the well-known ellipsometry equation:

$$\frac{\tilde{T}_p}{\tilde{T}_s} = \tan\psi \exp(i\Delta).$$

The ellipsometric angles and parameters of birefringence (BR) Δn and dichroism Δk are related in the following way:

$$\Delta n = n_{\parallel} - n_{\perp} = \frac{\lambda}{2\pi l}\Delta,$$

$$\Delta k = k_{\parallel} - k_{\perp} = -\frac{\lambda}{2\pi l}\ln(\tan\psi). \qquad (1)$$

Figures 1–3 present the transmission spectra and spectral dependences of birefringence and dichroism parameters at different magnetic field intensities. The BR spectra of the studied sample do not differ in any significant way from the spectra of aggregatively stable magnetic fluids with magnetite particles discussed earlier in [19,20]. At low field intensities, a maximum in the region of 470–480 nm and a minimum in the region 740–750 nm, which are also similar to those reported in [20], are seen in the dichroism spectrum. However, when the magnetic field intensity exceeds 10 kA/m, the shape of dichroism spectra changes

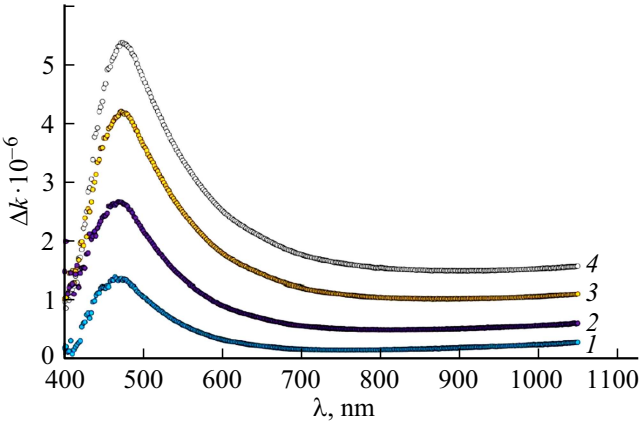

Figure 3. Spectra of dichroism in a magnetic fluid with a concentration of 0.05% at $H = 5$ (*1*), 9 (*2*), 13 (*3*), and 20 kA/m (*4*).

significantly. The dichroism parameter grows substantially throughout the visible and near-IR ranges. The most significant increase is observed in the 700–1000 nm region, and the minimum found in this region in weak fields becomes almost indiscernible.

The magnetic field also has a significant influence on the transparency spectra of a magnetic fluid. In zero field, the transmission spectra have a characteristic maximum in the 740–750 nm region, which is associated with features in the imaginary part of the refraction index spectrum of magnetite, and a faint minimum in the 910–930 nm region, which corresponds to the 3rd overtone of valence vibrations of methyl (CH_3) and methylene (CH_2) groups of hydrocarbon molecules in kerosene. As the magnetic field intensity increases to 20 kA/m, the maximum transparency value decreases by a factor of more than 2, and the transmission maximum in the 740–750 nm region becomes less pronounced. Figure 4 illustrates the effect of temperature on the transmission spectrum of a sample with a concentration of 0.05% in a magnetic field. An increase

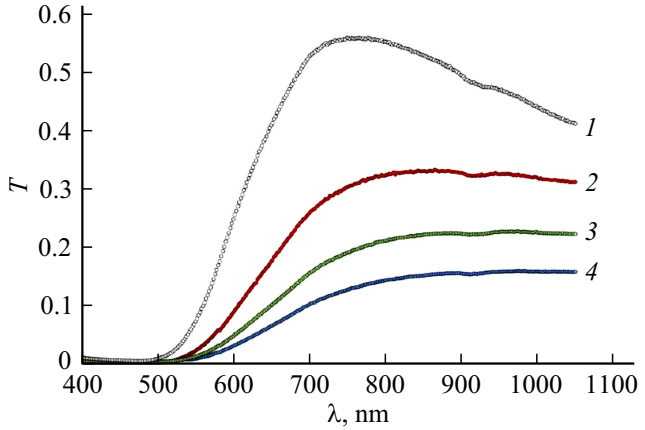

Figure 4. Effect of temperature on transmission spectra under the influence of a magnetic field: $H = 0$ and $T = 297$ K (*1*); $H = 26$ kA/m and $T = 285$ K (*2*), 297 K (*3*), and 313 K (*4*).

in temperature of the sample does, in a sense, neutralize changes in the spectra induced by a magnetic field. With an increase in temperature, the transparency of the sample in a magnetic field is restored partially, and the transmission maximum around 750 nm, which is hard to distinguish under the influence of a magnetic field at room temperature, becomes more noticeable. When the temperature drops to below-room levels, an even more profound reduction in transparency is observed throughout the entire spectral range, and the transparency maximum vanishes completely.

Discussion

The spectra of optical effects in aggregated magnetic fluids may be interpreted based on the assumption that complex refraction indices of a nanosized magnetite particle and an aggregate of such particles differ. As an aggregate grows in size in a magnetic field, the spectrum of its complex refraction index may change, and this will definitely affect the shape of spectra of optical effects. The effective medium model [21,22] is applicable in the characterization of optical parameters of an aggregate. With this approach, a nanoparticle aggregate is presented as a homogeneous continuous medium with effective permittivity $\tilde{\varepsilon}_a$, which is a complex quantity. Since the permeability of an aggregate at optical frequencies is $\mu = 1$, the relation between the effective permittivity and the complex refraction index of this aggregate is given by the known equation $\tilde{\varepsilon}_a = \tilde{n}_a^2 = (n_a + ik_a)^2$. The best-known effective medium approximations (Maxwell, Maxwell Garnett, and Bruggeman formulae) for matrix two-phase systems with spherical inclusions normally contain only three parameters: the volume concentration of inclusions and the permittivities of the inclusion and the surrounding medium. These expressions do not feature the size of inclusions, which limits their applicability in systems with a variable inclusion size. Modified effective medium models with the size of inclusions factored in were proposed in [23,24]. Following [24], we write the effective permittivity of an aggregate:

$$\varepsilon_a = \varepsilon_0 + \varepsilon_0 \frac{3C_V\alpha}{1 - C_V\alpha}\left\{1 + \left[\frac{11i}{10}\left(\frac{2\pi r_a}{\lambda}\right)^2 \mathrm{Im}\alpha + \right.\right.$$

$$\left.\left. + \frac{2i}{3}\left(\frac{2\pi r_a}{\lambda}\right)^3 \mathrm{Re}\alpha\right]\frac{1}{1 - C_V\alpha}\right\},$$

$$\alpha = \frac{m^2 - 1}{m^2 + 2}, \qquad (2)$$

where ε_0 is the permittivity of the medium surrounding the aggregate, r_a is the aggregate radius, C_V is the volume concentration of magnetite nanoparticles in the aggregate, and $m = n_m/n_0$ is the relative refraction index. Let us assume that the volume concentration of magnetite particles in the aggregate is $C_V \approx 33\%$, which corresponds to the maximum volume concentration of magnetite nanoparticles in a magnetic fluid when it loses fluidity.

Figure 5 presents the spectra of real and imaginary parts of the refraction index of a magnetite nanoparticle aggregate calculated in accordance with formula (2) for different sizes of the aggregate. The refraction index spectrum of nanosized magnetite ($n_m(\lambda)$) needed for calculations was taken from [19]. These calculations reveal that the spectrum of the real part of the refraction index changes little as the aggregate grows in size; the maximum of the spectrum just gets slightly lower and shifts toward longer wavelengths. The spectrum of the imaginary part of the refraction index undergoes much more substantial changes. In the visible region, the calculated imaginary part of the refraction index grows significantly with an increase in aggregate size (by a factor of more than 3 within the 500–700 nm range); in addition, if the aggregate is at least 50 nm in size, the characteristic minimum at 750 nm vanishes. As was demonstrated in [25], it is this minimum that induces a well-pronounced transparency maximum in the near-IR region of the transmission spectrum of magnetite-based magnetic fluids.

Let us use the method detailed in [19] to determine the optical characteristics of nanoparticle aggregates from experimental data. This method relies on measurements of BR and dichroism spectra and calculations of real and imaginary parts of the refraction index of colloidal particles performed using the following formulae [19]:

$$\Delta n = C_V \mathrm{Re}(B)\Phi(\sigma, \xi),$$

$$\Delta k = C_V \mathrm{Im}(B)\Phi(\sigma, \xi)). \qquad (3)$$

Here, C_V is the volume concentration of particles, $\Phi(\sigma, \xi)$ is the orientation function, and B is the parameter specified by the shape and optical characteristics of particles. The orientation function for magnetic particles with an arbitrary value of magnetic anisotropy σ is written as [26]

$$\Phi(\sigma, \xi) = \frac{3}{2}\left[1 - \frac{3L(\xi)}{\xi}\right]\left(\frac{d}{d\sigma}\ln R(\sigma) - \frac{1}{3}\right), \qquad (4)$$

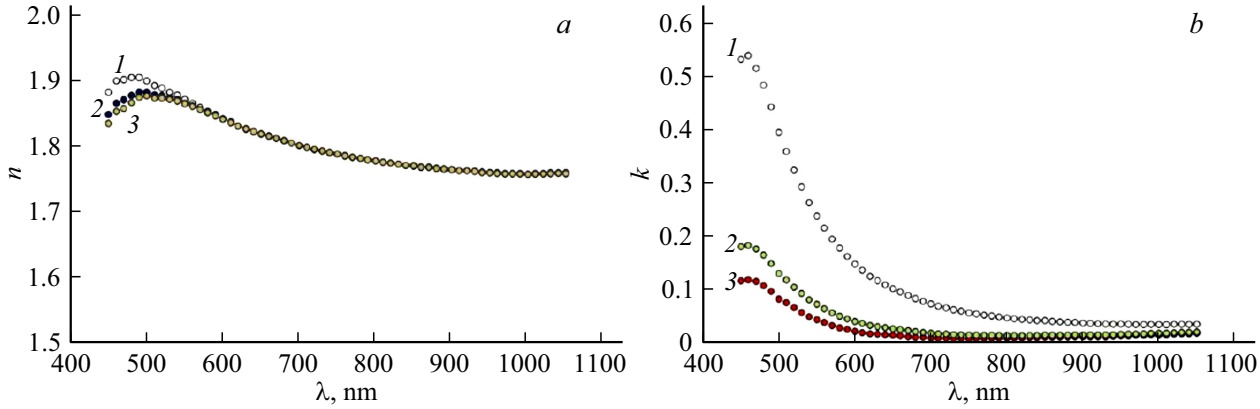

Figure 5. Results of calculations of real (*a*) and imaginary (*b*) parts of the effective refraction index of aggregates 30 (*1*), 50 (*2*), and 90 nm (*3*) in size.

where $\xi = \mu_0 m_0 H/kT$ and $\sigma = KV/kT$ are the ratios of the particle energy in a magnetic field and the energy of magnetic anisotropy to thermal energy; m_0 and V are the magnetic moment and the volume of a particle, respectively; and K is a constant incorporating the magnetic anisotropy of a magnetite crystal and the magnetic particle shape anisotropy. The second factor in (4) specifies the correction in the orientation function for superparamagnetic $\sigma \ll 1$ and magnetically hard $\sigma \gg 1$ single-domain particles:

$$\frac{3}{2}\left(\frac{d}{d\sigma}\ln R(\sigma) - \frac{1}{3}\right) = \begin{cases} \frac{2\sigma}{15}, & \sigma \ll 1 \\ 1 - \frac{3}{2\sigma}, & \sigma \gg 1 \end{cases}. \qquad (5)$$

The estimates of σ for magnetite particles with a radius of 13.7 nm demonstrate that they generally are magnetically hard ($\sigma \approx 70$); therefore, the corresponding factor in (4) may be considered close to unity. Similar reasoning remains valid for aggregates of such particles. The only parameter in (3) depending on the ratio of refraction indices of the colloidal particle material and the liquid dispersion medium ($m = n_1/n_0$) is B:

$$B = \frac{1}{2} n_0 (N_\perp - N_\parallel) \frac{Q^2}{(1 + QN_\perp)(1 + QN_\parallel)},$$

$$Q = m^2 - 1. \qquad (6)$$

Coefficients $N_\parallel$ and $N_\perp$ in Eq. (6) are the components of the depolarization tensor parallel and orthogonal to the principal axis of the particle, respectively. Orientation function $\Phi(\sigma, \xi)$ was determined from the field dependence of the magneto-optical effect normalized to its magnitude in the state of saturation: $\Delta n(H)/\Delta n_s = \Phi(\sigma, \xi)$. It is known that a correct magnitude of the optical effect in the state of saturation is rather hard to determine experimentally, since magnetic fields of a very high intensity (around 500 kA/m or even higher) are needed. The following approximation for the Langevin function at $\xi \gg 1$ was used to determine Δn_s:

$$1 - \frac{3L(\xi)}{\xi} \approx 1 - \frac{3}{\xi} + \frac{3}{\xi^2}. \qquad (7)$$

Figure 6 shows the dependence of the BR magnitude on the inverse field intensity. An approximation of the dependence in relatively strong magnetic fields by a second-order polynomial allows one to determine Δn_s from the limit magnitude of the effect at $1/H \to 0$ (i.e., in a field of a very high intensity).

The refraction index of aggregates of magnetite nanoparticles at different wavelengths λ_i was calculated by solving the following equations numerically:

$$\mathrm{Re}\left(\frac{Q(\lambda_i)^2}{(1 + Q(\lambda_i)N_\perp)(1 + Q(\lambda_i)N_\parallel)}\right) = \frac{2\Delta n(\lambda_i)}{C_V n_0(\lambda_i)(N_\perp - N_\parallel)\Phi(\sigma, \xi)}, \qquad (8)$$

$$\mathrm{Im}\left(\frac{Q(\lambda_i)^2}{(1 + Q(\lambda_i)N_\perp)(1 + Q(\lambda_i)N_\parallel)}\right) = \frac{2\Delta k(\lambda_i)}{C_V n_0(\lambda_i)(N_\perp - N_\parallel)\Phi(\sigma, \xi)}, \qquad (9)$$

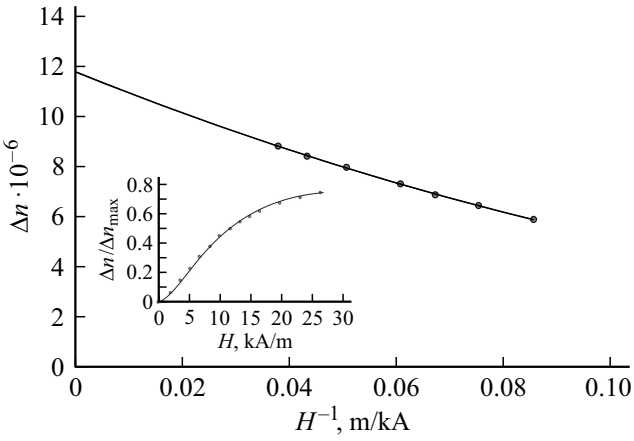

Figure 6. Determination of the BR magnitude in the state of saturation. The field dependence of orientation function Φ is shown in the inset.

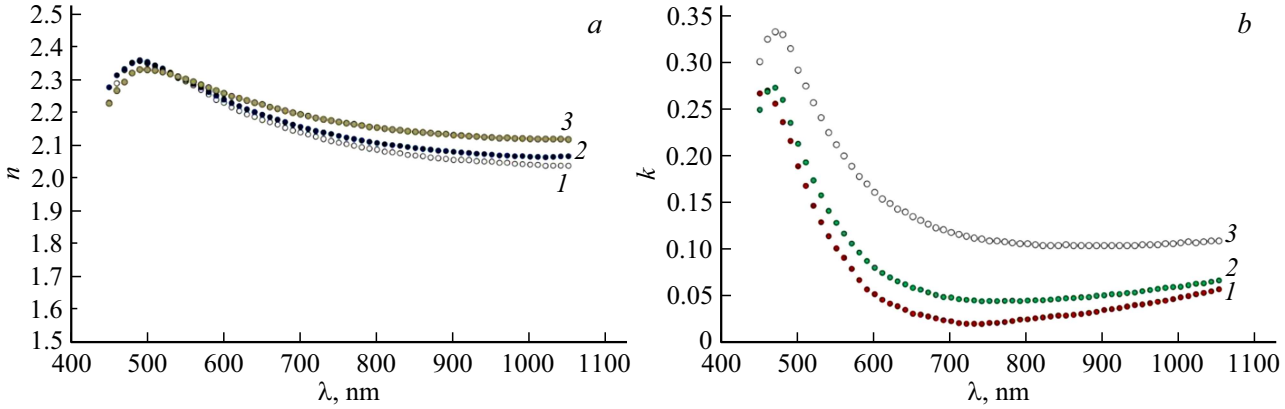

Figure 7. Spectra of real and imaginary parts of the refraction index of nanoparticle aggregates calculated based on the spectra of birefringence and dichroism effects at different magnetic field intensities: $H = 2$ (*1*), 6.7 (*2*), and 20 kA/m (*3*).

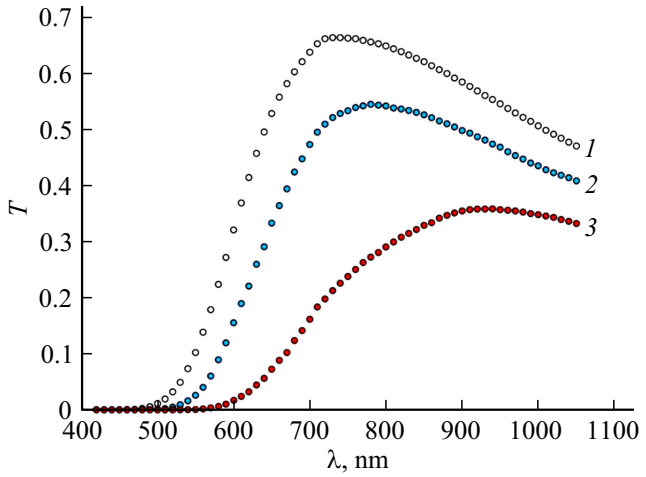

Figure 8. Results of calculations of transmission spectra of a magnetic fluid without nanoparticle aggregates (*1*) and with aggregates 50 (*2*) and 90 nm (*3*) in size.

where $\Delta n(\lambda_i)$ and $\Delta k(\lambda_i)$ are the experimental values of birefringence and dichroism parameters measured at wavelength λ_i.

Figure 7 presents the spectra of real and imaginary parts of the refraction index of nanoparticle aggregates determined based on the spectral dependences of BR and dichroism at different intensities of a permanent magnet field. The obtained spectra of optical parameters of aggregates agree closely with the results of calculations in accordance with the effective medium model (Fig. 5). The characteristic minimum in the spectrum of the imaginary part of the refraction index becomes less pronounced as the field intensity increases. A comparison of calculated spectra and those plotted based on experimental data suggests that the shape of the spectrum of the refraction index of a magnetite nanoparticle aggregate changes significantly in the process of its growth.

Let us demonstrate that changes in the size of an aggregate and the spectrum of its refraction index may account for the specific features of the transmission spectra of a magnetic fluid under the influence of a magnetic field (see Fig. 1). Since the concentration of nanoparticles and aggregates in the samples was low, the Bouguer–Lambert equation may be used to calculate transmission spectra:

$$T(\lambda) = \exp[-(\sigma_0(\lambda)N + \sigma_a(\lambda)N_a)l], \qquad (10)$$

where N, N_a, σ_0, and σ_a are the number concentrations and light attenuation cross sections of individual nanoparticles and aggregates, respectively. Owing to the fact that aggregates in a magnetic fluid range in size from several tens to hundreds of nanometers, the Rayleigh approximation is inapplicable in calculations of light attenuation cross section σ_a. Instead, one should use a more rigorous theory for particles with sizes close to the wavelength of visible light: the Mie theory. It should also be taken into account that the volume concentration of magnetite in the sample remains unchanged in the process of particle aggregation. The number concentrations of individual nanoparticles and aggregates are then bound by the following relations: $N = (1 - f)N_0$ and $N_a = fN_0r_0^3/r_a^3$, where f is the fraction of particles incorporated into aggregates (degree of aggregation); r_0 and r_a are the radii of an individual particle and an aggregate, respectively; and $N_0 = 3C_V/(4\pi r_0^3)$ is the number concentration of nanoparticles without aggregation. Figure 8 presents the results of calculations of transmission spectra by formula (10) for a non-aggregated magnetic fluid and a fluid containing aggregates 50 and 90 nm in size. The degree of particle aggregation was set to 10% in these calculations. The calculated spectra are in a very good qualitative agreement with experimental data (Fig. 1). A certain quantitative discrepancy in transparency values may be attributed to the relative simplicity of the calculation model, which does not take into account the polydispersity and polymorphism of particles and aggregates and variations of the degree of particle aggregation during the growth of aggregates. The dependence of the spectrum of the complex refraction index on the size of aggregates is the reason why the transmission spectra of a magnetic fluid vary with

temperature (Fig. 4). As was demonstrated in [26], the average size of aggregates in real polydisperse magnetic colloids is determined by a complex balance of influence of a magnetic field and temperature. In general, an increase in temperature leads to a reduction in the average size of aggregates; as a result of this, the transmission spectrum in a magnetic field becomes closer to the spectrum in zero field. A reduction in temperature has the opposite effect.

Conclusion

The formation of aggregates of magnetite nanoparticles in a magnetic fluid induces significant changes in the spectra of optical effects. One of the most interesting features is the change in the shape of transmission spectra of a magnetic fluid. This involves not only a reduction of the overall transparency of the sample, but also the vanishing of the transmission maximum in the 740−750 nm region. Significant changes are also observed in the dichroism spectrum of aggregatively unstable magnetic fluids. In this case, an increase in dichroism in the long-wavelength visible region and the near-IR region is coupled with smearing of the effect minimum, which becomes unpronounced. The interpretation of these features is based on changes in the spectra of the complex refraction index of aggregates occurring during their growth. The calculated (within the effective medium model) spectra of real and imaginary parts of the refraction index of aggregates of different sizes agree closely with those plotted based on experimental data. Calculations of the transmission spectra of aggregated magnetic fluids with the use of experimental dependences of the refraction index spectrum also provide a fine qualitative and quantitative agreement with experiments. The effect of temperature on the transmission spectra of magnetic fluids was attributed to the dependence of spectra of the complex refraction index of aggregates on temperature and their average size.

Funding

The study was supported by the Ministry of Education and Science of the Russian Federation under the state research assignment (FSRN-2023-0006).

Conflict of interest

The authors declare that they have no conflict of interest.

References

[1] E.Ya. Blums, M.M. Maiorov, A.O. Cebers. *Magnetic Fluids* (Walter de Gruyter, Berlin, 1997).
[2] J. Phillip. Adv. Colloid Interface. Sci., **311**, 102810 (2023). DOI: 10.1016/j.cis.2022.102810
[3] H.W. Davies, J.P. Llewellyn. J. Phys. D.: Appl. Phys., **13**, 2327 (1980). DOI: 10.1088/0022-3727/13/12/018
[4] B.R. Jennings, M. Xu, P.J. Ridler. Proc. Royal Soc. A., **456**, 891. (2000). DOI: 10.1098/rspa.2000.0541
[5] F. Donatini, S. Neveu, J. Monin. J. Magn. Magn. Mater., **162**, 695 (1996). DOI: 10.1016/0304-8853(96)00083-2
[6] C.V. Yerin, V.I. Vivchar. J. Magn. Magn. Mater., **498**, 166144 (2020). DOI: 10.1016/j.jmmm.2019.166144
[7] R.V. Mehta, Rajesh Patel, R.V. Upadhyay. Phys. Rev. B., **74**, 195127 (2006). DOI: 10.1103/PhysRevB.74.195127
[8] K.V. Erin. Opt. Spectrosc., **120** (2), 320 (2016). DOI: 10.1134/S0030400X16020090.
[9] M.V. Avdeev, V.L. Aksenov. Physics-Uspekhi, **53** (10), 971 (2010). DOI: 10.3367/ufne.0180.201010a.1009.
[10] R.V. Mehta, R.V. Upadhyay, Rajesh Patel, Premal Trivedi. J. Magn. Magn. Matter., **289**, 36 (2005). DOI: 10.1016/j.jmmm.2004.11.011
[11] A.O. Ivanov, S.S. Kantorovich. Phys. Rev. E., **70**, 021401 (2004). DOI: 10.1103/PhysRevE.70.021401
[12] M. Rusanov, V. Zverev, E. Elfimova. Phys. Rev. E., **104**, 044604 (2021). DOI: 10.1103/PhysRevE.104.
[13] A.S. Ivanov. J. Magn. Magn. Mater., **441** (10), 620 (2017). DOI: 10.1016/j.jmmm.2017.06.059
[14] C. Rablau, P. Vaishnava, C. Sudakar, R. Tackett, G. Lawes, R. Naik. Phys. Rev. E. **78**, 051502 (2008). DOI:10.1103/PhysRevE.78.051502
[15] C.V. Yerin, V.I. Vivchar. J. Magn. Magn. Mater., 171437 (2023). DOI: 10.1016/j.jmmm.2023.171437
[16] J. Ge, Y. Hu, Y. Yin. Angewandte Chemie Int. Ed., **46** (39), 7428 (2007). DOI: 10.1002/anie.200701992
[17] J. Philip, V. Mahendran, L.J. Felicia. J. Nanofluids, **2**, 112 (2013). DOI: 10.1166/jon.2013.1050
[18] S. Han, S. Pu, Z. Hao et al. Opt. Lett., **48**, 4504 (2023). DOI: 10.1364/OL.499780
[19] K.V. Yerin. Inorganic Materials, **58** (4), 403 (2022). DOI: 10.1134/S0020168522040045.
[20] C.V. Yerin, V.I. Vivchar, E.I. Shevchenko. Bull.Russian Acad. Sci.: Phys., **87** (3), 272 (2023). DOI: 10.3103/S1062873822701064.
[21] A.S. Shalin. Quantum Electronics, **40** (11), 1004 (2010). DOI: 10.1070/QE2010v040n11ABEH014330.
[22] L.A. Golovan, V.Yu. Timoshenko, P. Kashkarov. Physics-Uspekhi, **50** (6), 595 (2007). DOI: 10.1070/PU2007v050n06ABEH006257.
[23] B.A. Belyaev, V.V. Tyurnev J. Experim. and Theor. Phys., **127** (4), 608 (2018). DOI: 10.1134/S1063776118100114.
[24] C.-A. Guérin, P. Mallet, A. Sentenac. J. Opt. Soc. Am., **A 23**, 349 (2006). DOI: 10.1364/JOSAA.23.000349
[25] K.V. Yerin, V.I. Vivchar. J. Appl. Spectr., **90** (6), 1205 (2024). DOI: 10.1007/s10812-024-01654-7.
[26] A.S. Ivanov *Gidrodinamika kapel'nykh agregatov i nemagnitnykh tel, pogruzhennykh v magnitnuyu zhidkost'*. Doctoral Dissertation in Mathematics and Physics (Inst. Mekh. Sploshnykh Sred, Perm, 2023) (in Russian). URL: https://permsc.ru/images/docs/disser/D.004.036.01/Ivanov_AS/abstract_ias.pdf

Translated by D.Safin